Cell, Vol. 100, 469–478, February 18, 2000, Copyright ©2000 by Cell Press

Regulation of Auxin Response by the Protein Kinase PINOID

Sioux K. Christensen,* Nicole Dagenais,* Joanne Chory,*†‡ and Detlef Weigel*
*Plant Biology Laboratory
†Howard Hughes Medical Institute
The Salk Institute for Biological Studies
10010 North Torrey Pines Road
La Jolla, California 92037

Summary

Arabidopsis **plants carrying mutations in the** ***PINOID*** **(*PID*) gene have a pleiotropic shoot phenotype that mimics that of plants grown on auxin transport inhibitors or of plants mutant for the auxin efflux carrier** ***PINFORMED*** **(*PIN*), with defects in the formation of cotyledons, flowers, and floral organs. We have cloned** ***PID*** **and find that it is transiently expressed in the embryo and in initiating floral anlagen, demonstrating a specific role for** ***PID*** **in promoting primordium development. Constitutive expression of** ***PID*** **causes a phenotype in both shoots and roots that is similar to that of auxin-insensitive plants, implying that** ***PID*****, which encodes a serine-threonine protein kinase, negatively regulates auxin signaling.**

Introduction

From its point of synthesis at the plant apex (Davies, 1995), the phytohormone auxin is directionally transported through the plant body to effect an astonishing variety of morphological processes. Auxin is required early in development to establish the bilateral axis of the developing embryo (Sciavone and Cooke, 1987; Liu et al., 1993; Fischer and Neuhaus, 1996; Hadfi et al., 1998). Later, auxin participates in vascular element patterning and differentiation (Aloni, 1995), lateral organ outgrowth in the root and shoot (Okada et al., 1991; Celenza et al., 1995), and local growth responses to external stimuli such as light and gravity (Kaufman et al., 1995).

While an understanding of the mechanisms of auxin action at the molecular level is preliminary, genetic and biochemical approaches have begun to reveal discrete aspects of auxin transport, signaling, and response. Two related *Arabidopsis* proteins, PIN and EIR1/AGR1/PIN2, which share homology with bacterial membrane transporters, function as auxin efflux carriers in the shoot and root, respectively (Chen et al., 1998; Gälweiler et al., 1998; Luschnig et al., 1998; Müller et al., 1998). The auxin influx carrier AUX1, which shares homology with plant and fungal amino acid permeases, functions in root gravitropism (Bennett et al., 1996; Marchant et al., 1999). *TIR3* has been implicated in auxin transport in both the root and the shoot. *tir3* mutants have fewer binding sites than wild type for the auxin transport inhibitor NPA (α-naphthylphthalamic acid), suggesting that the *TIR3* gene product either encodes or regulates an NPA-binding protein (Ruegger et al., 1997). An auxin receptor has not been unambiguously identified, but overexpression of the auxin-binding protein ABP1 affects cell expansion, a transcription-independent auxin-regulated process (Jones et al., 1998).

Apart from proteins involved in auxin transport and binding, several classes of auxin-signaling molecules have been identified. One class includes regulators of protein stability such as AXR1 and TIR1. TIR1 is an F box protein that together with SKP1 and Cdc53 constitutes an E3 ubiquitin ligase complex (Patton et al., 1998; Gray et al., 1999). AXR1 is a component of the RUB conjugation pathway, which leads to RUB modification of the Cdc53 subunit of the E3 complex itself (Lammer et al., 1998; Liakopoulos et al., 1998).

Another class of auxin signaling molecules comprises the ARF and Aux/IAA families of transcription factors (Guilfoyle et al., 1998). In vitro homodimerization and heterodimerization within each family, as well as interactions between the families, suggest that combinatorial action of these proteins confers cell or tissue specificity in auxin response (Kim et al., 1997; Ulmasov et al., 1997a, 1997b, 1999). Although ARFs and Aux/IAAs were initially identified by biochemical methods, several *Arabidopsis* mutants with defects in auxin signaling have subsequently been shown to carry lesions in *ARF* or *Aux/IAA* genes (Hardtke and Berleth, 1998; Rouse et al., 1998; Tian and Reed, 1999). One example is the *MP* gene, which encodes ARF5 and whose loss of function in the shoot results in a pin-like inflorescence similar to that seen in *pin* mutants, or in plants treated with polar auxin transport inhibitors (Okada et al., 1991; Berleth and Jürgens, 1993).

A third mutant with a pin-like inflorescence is *pid* (Bennett et al., 1995). In contrast to *pin* and *mp* mutants, which have substantially decreased auxin flow in the inflorescence, *pid* mutants show only a modest reduction in polar auxin transport (Okada et al., 1991; Bennett et al., 1995; Przemeck et al., 1996). Here we report that *PID* encodes a member of a plant-specific serine-threonine protein kinase family. In contrast to *PIN* and *MP*, which are expressed in the vasculature of the inflorescence stem as well as in developing primordia, *PID* is predominantly expressed in anlagen of lateral primordia, consistent with *PID* affecting downstream events in auxin signaling. Moreover, *PID* overexpression results in shoot and root phenotypes similar to those of auxin-insensitive mutants, indicating that PID negatively regulates auxin signaling.

Results

Expression of Meristem Markers in *pid* Inflorescences

The pin-like inflorescence of *pid* mutants suggests that *PID* is required either to regulate patterning within the

‡To whom correspondence should be addressed (e-mail: chory@salk.edu).

shoot apical meristem, or more specifically to direct lateral meristem formation. To distinguish between these possibilities, we examined the expression of several genes that are expressed in the developing inflorescence or in emerging floral primordia. *CLV1* and *UFO* are expressed in a complementary pattern in the shoot apex: *CLV1* is expressed in subepidermal layers at the center of the apex in the region corresponding to the meristem proper (Clark et al., 1997), while *UFO* is expressed in a cup-shaped region surrounding the meristematic core of the apex (Lee et al., 1997; Long and Barton, 1998). The expression of both genes in the apical meristem of *pid* mutant pins was similar to that seen in wild-type plants (Figures 1A–1D).

MP and *FIL* were used to examine lateral meristem formation in the *pid* inflorescence. *MP* is normally strongly expressed in floral anlagen and emerging flowers and more weakly in the developing vasculature (Hardtke and Berleth, 1998). *FIL* is expressed in a small abaxial domain in the flower anlagen and emerging floral primordia (Sawa et al., 1999; Siegfried et al., 1999). *MP* was strongly expressed in *pid* apices along with weaker expression in the developing vasculature (Figure 1F). While *FIL* RNA was detected in *pid* mutants, *FIL* was only weakly expressed in discrete foci on the flanks of the inflorescence apex, indicating that early development of lateral primordia was defective in *pid* mutants (Figure 1H).

Because of the similar *pid* and *pin* mutant phenotypes, we also investigated *PIN* expression. In wild type, *PIN* is expressed in both the vasculature (Gälweiler et al., 1998) and in developing flowers (Figure 1I), similar to the *MP* expression domains. In *pid* mutants, *PIN* was expressed in a small group of cells on the flanks of the shoot apical meristem and in the procambium (Figure 1J), in a pattern similar to that observed in wild-type plants.

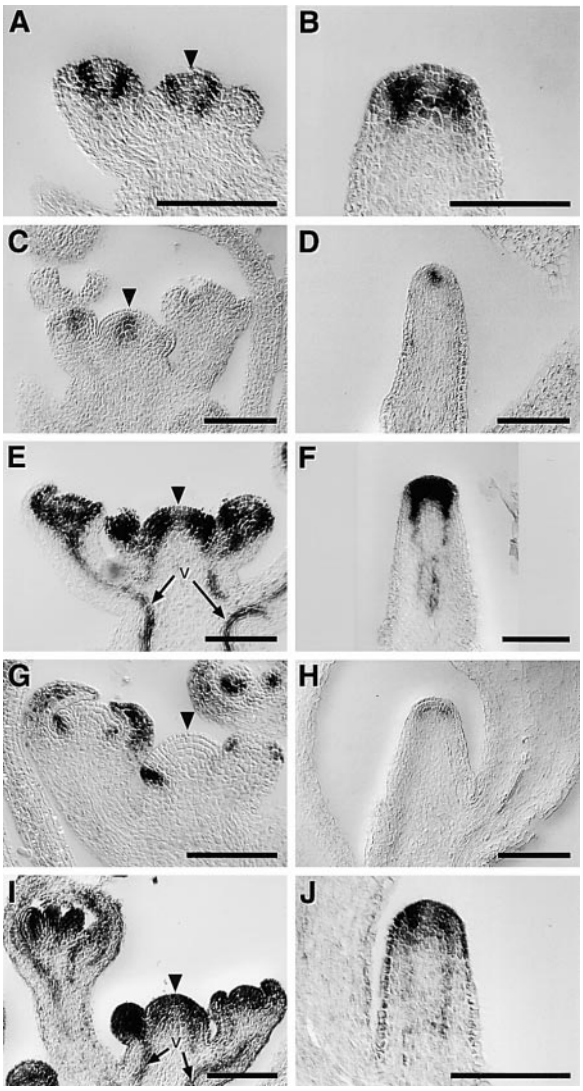

Figure 1. Expression of Marker Genes in Wild-Type and *pid-9* Inflorescences

Left panels shows inflorescence apices of wild type, and right panels show *pid-9* pin-like inflorescences. Arrowheads indicate the center of the shoot meristem proper in wild type. The provascular strands that express *MP* and *PIN* are indicated as well (v). (A and B) *UFO*. (C and D) *CLV1*. (E and F) *MP*. (G and H) *FIL*. (I and J) *PIN*. Scale bars are 100 μm.

Petal and Carpel Venation in *pid* Mutants

Auxin signaling controls vascular patterning in the cotyledons, leaves, stems, and flowers of *Arabidopsis* (Sessions and Zambryski, 1995; Przemeck et al., 1996; Gälweiler et al., 1998; Mattsson et al., 1999). Because of the similar inflorescence phenotype of *pid* mutants with those of plants mutant for the auxin transporter *PIN* and the ARF *MP*, which are required for vascular patterning (Gälweiler et al., 1998; Mattsson et al., 1999), we investigated whether this aspect of auxin response was disrupted in *pid* mutants as well. While the venation of nonfloral tissues including cotyledons, rosette leaves, and inflorescence stems was normal in *pid* mutants (data not shown), vascular elements within the *pid* flower were abnormal.

Two female reproductive organs, the carpels, form the central gynoecium of the *Arabidopsis* flower (Smyth et al., 1990). Its primary vascular system is composed of four vascular bundles that run parallel to its longitudinal axis (Sessions and Zambryski, 1995). One lateral bundle runs the length of each valve, which makes up the outer wall of the ovary, and terminates just below the junction between valve and style. The two opposing medial bundles arise in the margins of the septum, which bisects the gynoecium and forms the inner wall of the ovary. Within the ovary, lateral branches of the medial bundles supply the individual ovules. After entering the style, immediately distal to the valves, each medial bundle branches to form a fan of xylem on the medial face of the style (Figure 2A).

The weak allele *pid-8* had variable defects characterized by reduced valve formation and distal displacement of valve tissues. *pid-8* gynoecia frequently developed only a single carpel, and the lateral vascular bundle that normally supplies the missing valve was deleted (Figure 2B). In the reduced valve tissues, primary and secondary lateral vascular elements differentiated normally. Despite the relatively normal morphology of these valves, *pid-8* gynoecia frequently lacked ovular xylem (Figure

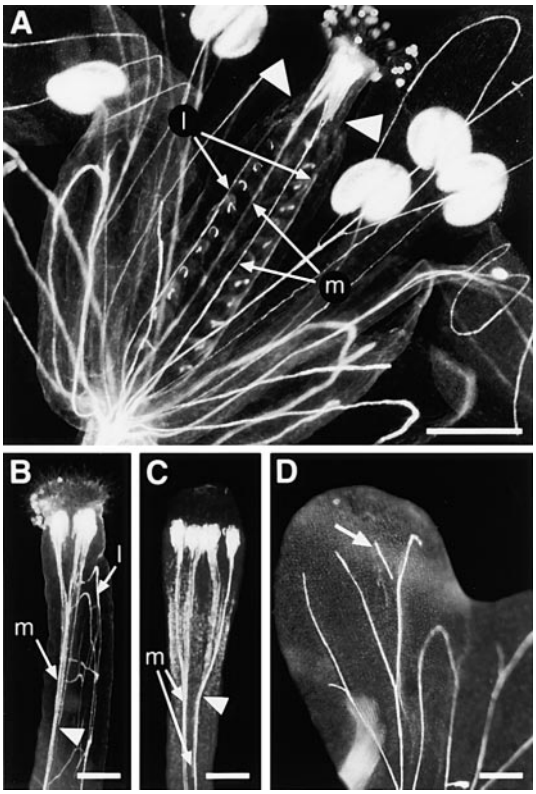

Figure 2. Venation Patterns in Wild-Type and *pid* Flowers

(A) Medial view of a wild-type flower showing the two lateral (l) and two medial (m) vascular bundles of the gynoecium. The medial bundles branched at the junction between valve and style (arrowhead) and formed fans of xylem on the medial face of the style.

(B) Medial view of a *pid-8* gynoecium comprising a single carpel, which consists of a single valve and a single lateral bundle. The medial bundles began to branch before they entered the style (arrowhead), and the xylem fans have formed on the lateral face of the style.

(C) *pid-9* gynoecium. Valves and lateral bundles are absent. The two medial bundles have branched repeatedly to form several xylem fans around the tip of the gynoecium.

(D) A fused *pid-9* petal with a detached vascular element (arrow). Scale bars are 50 μm in (A), and 20 μm in (B)–(D).

2B). Regardless of valve number, we consistently observed two medial xylem bundles. However, these bundles branched prematurely, proximal to the valve/style junction, and the vascular fans formed on the lateral, rather than the medial face of the style.

In the few flowers that formed in strong *pid-9* mutants, valves were usually replaced by tissue that resembled wild-type style. Consistent with this replacement, lateral vascular bundles were missing. As in the weak *pid-8* allele, medial bundles differentiated normally, but branched prematurely, close to the midpoint of the reduced *pid-9* gynoecium. This premature branching resulted in the formation of supernumerary xylem fans that encircled the distal tip of the gynoecium (Figure 2C). In addition to defects in the carpel, *pid-9* petals occasionally showed defects in vascular continuity, and the vascular loops characteristic of wild-type petals were often replaced by linear veins that terminated near the petal margin (Figure 2D).

PID Encodes a Serine-Threonine Protein Kinase

The recessive *pid-9* mutant was isolated from a T2 population of plants transformed with the activation-tagging vector pSKI015 (Weigel et al., 2000). Segregation analysis revealed that the *pid-9* mutation was closely linked to the T-DNA insertion. Plant DNA flanking the left and right borders of the insertion was recovered by plasmid rescue and sequenced. The T-DNA in *pid-9* was found to be inserted in the genomic sequence represented in BAC T31E10, whose position on the physical map correlated closely with the genetic map position of *PID* on chromosome II (Bennett et al., 1995).

The T-DNA insertion in *pid-9* disrupted the coding region of an annotated gene (accession AAC26704) with a single intron. We did not find a cDNA in 600,000 clones of a floral cDNA library (Weigel et al., 1992), indicating that transcripts of this gene are rare. The gene structure predicted from the genomic sequence was confirmed by reverse transcription followed by polymerase chain reaction. To establish that this gene represented the *PID* locus, we sequenced the coding region of this gene in twelve *pid* mutant alleles. For each allele, a mutation was found in the gene disrupted by the *pid-9* T-DNA. These lesions included two nonsense mutations, nine missense mutations, and one small deletion (Table 1; Figure 3A).

The predicted PID protein of 438 amino acids shares extensive similarity with several classes of serine-threonine protein kinases (Figure 3A). The homology of PID to the catalytic domain of protein kinases extends the length of the predicted protein and contains all eleven subdomains typical of protein kinases (Hanks et al., 1988). Comparison of PID with the consensus sequence derived from yeast and animal protein kinases revealed that PID contained 13 of the 14 invariant amino acids that define the catalytic domain. The single exception was the replacement of an invariant glycine at position 225 with aspartate, changing the conserved DFG motif to DFD. A stretch of approximately 50 amino acids between the conserved subdomains VII and VIII may represent a regulatory domain. All but one of the missense mutations were either in, or within two amino acids from, one of the kinase-typical invariant residues.

To determine whether PID is a functional protein kinase, we expressed the protein as a GST fusion product in *E. coli*. To examine the importance of specific residues within the kinase domain, and of the potential regulatory region between domains VII and VIII, we also expressed several PID derivatives generated by site-directed mutagenesis. As a negative control, Asp-205 was replaced with Ala, inactivating the ATP binding domain (GST:MPID). The importance of the DFD as opposed to the canonical DFG motif was addressed with a change of Asp-225 to Gly in GST:DFG. Finally, two fusion constructs were made to test the function of serines and threonines adjacent to the potential regulatory domain, by introducing negatively charged glutamate residues, which mimic phosphoserine or phosphothreonine. GST:ALT contained a Thr-294 to Glu substitution, and GST:ALS contained Glu substitutions at both Ser-288 and Ser-290.

The wild-type fusion, GST:PID, autophosphorylated in vitro (Figure 3B), while the GST:MPID fusion protein

Table 1. Sequence Changes in *pid* Alleles

Allele	Effect	Strain[a]	Origin	Codon Change	Amino Acid Change
1	strong	Ler	Bennett et al., 1995	CGA→TGA	R53stop
2	intermed.	Ler	Bennett et al., 1995	GGG→AGG	G380R
3	strong	Col	Bennett et al., 1995	CTC→TTC	L226F
4	strong	Ler	Bennett et al., 1995	AGA→AAA	R378K
5	strong	Ler	Bennett et al., 1995	GAG→AAG	E128K
6	strong	Ler	Bennett et al., 1995	CGA→TGA	R63stop
7	strong	Ler	Bennett et al., 1995	38 bp Δ (964 to 1001)	truncation after L321
8	weak	Ws-2	Bennett et al., 1995	CCA→CAA	P300Q
9	strong	Col	This study	23 bp Δ (526-548); T-DNA insertion	truncation after R175
10	intermed.	No-0	Jennifer Fletcher	GGC→AGC	G84S
11	strong	Col	Ray Hong	GAG→AAG	E128K
12	strong	Col	Allen Sessions	AGA→AAA	R378K
13	weak	Ws-2	Allen Sessions	CAC→TAC	H166Y

[a] Ler, Landsberg *erecta*; Col, Columbia; Ws-2, Wassilewskija-2; No-0, Nossen.

was inactive. Both GST:ALS and GST:DFG autophosphorylated, with an apparent increase in activity in GST:DFG relative to wild-type GST:PID. GST:ALT did not show any autophosphorylation, indicating that it was either inactive, or that Thr-294 is the major autophosphorylation site.

Expression Pattern of *PID*

pid mutants exhibit morphological defects at both early and late stages of development. In wild type, two opposing cotyledons are formed during embryogenesis, and their position dictates the arrangement of the first pair of true leaves, which normally form perpendicularly to the cotyledons. *pid* mutants often develop three symmetrically arranged cotyledons, followed by three primary leaves that arise between the cotyledons. The rest of the vegetative shoot system develops normally in *pid* mutants. Defects become apparent again after the switch to the reproductive phase, when *PID* is required for floral meristem outgrowth and floral organ development (Bennett et al., 1995).

To determine whether these stage-specific phenotypes correlated with the temporal expression pattern of *PID* transcripts, and to determine where in the embryo and shoot *PID* acts to control morphogenesis, we examined *PID* RNA accumulation by in situ hybridization. The earliest point at which *PID* expression was detectable was during the globular stage of embryogenesis. *PID* was initially expressed on the apical flanks of the embryo, where the cotyledons will subsequently form (Figure 4A). Expression in the cotyledons persisted throughout the heart (Figure 4B) until the midtorpedo stage. By the bent-cotyledon stage, *PID* expression was only weakly detected in the apical meristem (Figure 4C).

Similarly, *PID* was only weakly expressed in the shoot apex and in young leaves of vegetatively growing plants (Figure 4D). *PID* RNA levels increased after the transition to reproductive development, although overall levels were low in comparison to those of other auxin-related genes such as *PIN* or *MP*. In the inflorescence, *PID* was expressed in discrete groups of cells on the flanks of the apex (Figures 4E and 4F), which initially marked the floral anlagen. As soon as floral primordia became morphologically distinct, *PID* RNA became restricted to the adaxial portion of the primordia. The initial expression pattern of *PID* in stage 3 flowers, which were about to form sepals, mimicked that of the expression pattern in the shoot apex (Figure 4G). In developing flowers, *PID* was transiently expressed in nascent floral organs (Figure 4H). As floral organs matured, *PID* transcripts were downregulated (not shown).

Because *pin* and *pid* mutants have similar inflorescence phenotypes, we examined *PID* expression in *pin-1* mutants. *PID* was weakly expressed at the flanks of the apex in *pin-1* mutants, indicating that changes in auxin levels in *pin-1* mutants did not affect *PID* expression (Figure 4I).

Consequences of Ectopic PID Expression

To determine whether PID is limiting for auxin signaling, we expressed the *PID* cDNA under the control of the CaMV 35S promoter, which is constitutively active in most plant tissues (Odell et al., 1985). Nine of 170 primary *35S::PID* transformants had a phenotype different from that of wild-type plants (Figures 5A, 5C, and 5E). Northern analysis of total RNA prepared from transgenic plants with this new phenotype and from transgenic plants that were phenotypically normal confirmed that *PID* was overexpressed only in the former (Figure 5B). As a control, we transformed plants with the *35S::MPID* construct, which lacked in vitro kinase activity. Of 126 T1 plants, none showed the *35S::PID* phenotype, indicating that PID functions as a protein kinase in vivo. Northern analysis of RNA prepared from pooled *35S::MPID* plants confirmed that levels of transcripts from the transgene were several fold higher than those from the endogenous locus, although transcript levels were lower than those observed for the wild-type construct. T1 individuals with a phenotype similar to that of *pid* loss-of-function mutants, indicating cosuppression, were found at similar frequency in *35S::PID* and *35S::MPID* transformants, confirming activity of the transgene in both sets of plants.

Hemizygous *35S::PID* plants were small and had dark green, curled leaves (Figure 5C). Eight of the nine T1 plants with vegetative defects also showed defects during the reproductive phase, with reduced apical dominance and reduced internode elongation. Four of these

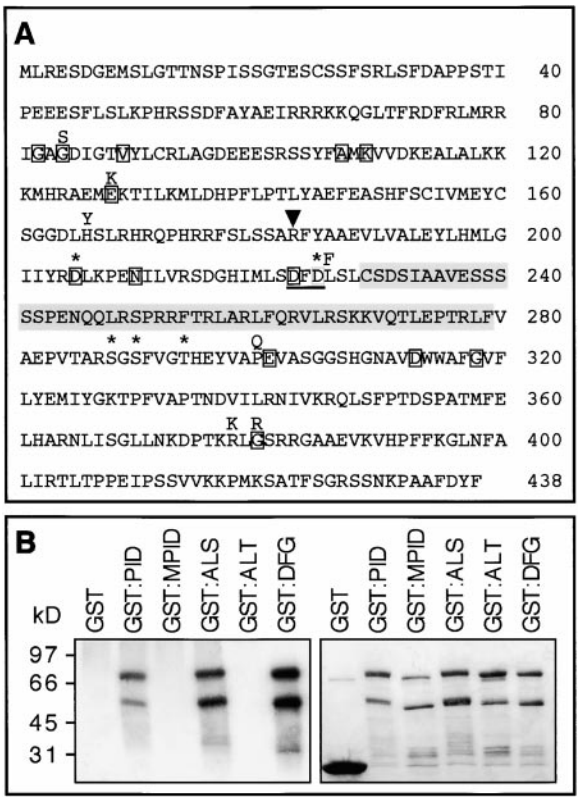

Figure 3. Structure and In Vitro Activity of PID Protein

(A) Deduced amino acid sequence of PID. Amino acid changes above the sequence indicate residues changed in *pid* alleles (Table 1), and asterisks indicate residues modified by site-directed mutagenesis in PID expression constructs (see text). Boxes indicate invariant protein kinase residues. The DFD in place of the canonical DFG motif is underlined. A putative regulatory domain is shaded. An arrowhead indicates the location of the single intron.

(B) In vitro autophosphorylation of PID. Bacterially produced GST-PID fusion protein and derivatives were incubated with [γ-^{32}P]ATP and separated by PAGE. Left panel shows an autoradiogram, right panel shows the same gel stained with Coomassie blue. The full-length fusion proteins are represented by the lower mobility bands.

T1 plants were sterile, while the other four plants were semifertile. Despite the severe morphological defects in the shoot system of *35S::PID* plants, which were reminiscent of those seen in auxin-insensitive and auxin-resistant plants (Lincoln et al., 1990), the vasculature of rosette leaves was largely normal (data not shown), indicating that *PID* overexpression did not equally affect all auxin-regulated processes.

One *35S::PID* line was chosen for further characterization. In the T2 progeny of this line a more severe phenotypic class was observed, consisting of extreme dwarves. These plants constituted approximately 10% of the T2 progeny and were sterile. Of the fertile T2 plants, two-thirds (139/207) carried the kanamycin resistance marker of the transgene and showed the same phenotype as the T1 parent, while the remaining third (68/207) was phenotypically wild type and sensitive to kanamycin. Segregation analysis of T3 progeny of twelve fertile T2 plants confirmed that each T2 plant had been hemizygous for the transgene, suggesting that the extreme dwarves had been homozygous. Since homozygous progeny were apparently underrepresented, it was likely that the majority of homozygous plants died as embryos, or failed to germinate.

Although *PID* is not required for normal root growth (D. Smyth, personal communication), we wondered whether ectopic expression of *PID* could affect auxin-regulated processes in the root as well. Two such processes have been particularly well studied using *Arabidopsis* mutants, namely gravitropism and lateral root initiation (Maher and Martindale, 1980; Lincoln et al., 1990; Bennett et al., 1996; Leyser et al., 1996; Ruegger et al., 1997; Chen et al., 1998; Luschnig et al., 1998; Müller et al., 1998; Tian and Reed, 1999), and *PID* overexpression affected both of them. *35S::PID* plants had either no or very few lateral roots, and roots grew aberrantly across the surface of the substrate instead of into it. The aberrant root growth was due to lack of a gravitropic response, as determined by growing segregating T2 progeny without selection on vertical plates. After 18 days, 15 of 24 T2 germinated seedlings had no lateral roots, and two seedlings had one lateral root. The remaining seven plants generated an average of ten lateral roots (range 4–16). Primary root growth in seedlings lacking lateral roots was random with respect to the gravity vector, while seedlings with more than one lateral root responded normally (Figure 5D), indicating that the lateral root defect and the gravitropic defect were genetically linked.

To determine whether the loss of lateral root formation in *35S::PID* plants could be bypassed by exogenous auxin, T2 plants were grown on plates supplemented with the synthetic auxin-analog NAA. After 10 days on 0.1 μm NAA, 11 of 37 germinated seedlings had produced an average of 24 lateral roots (range, 18–31), while the remaining 26 had failed to produce lateral roots, indicating that NAA did not overcome the block in lateral root formation caused by *PID* overexpression. As in the previous experiment, there was a perfect correlation between loss of lateral root formation and agravitropic root growth.

The failure of *35S::PID* plants to develop lateral roots in response to exogenous auxin can be explained by defects in either auxin uptake or response. To distinguish between these possibilities, we grew *35S::PID* and wild-type plants on plates containing 0, 0.1, 0.5, or 1.0 μM NAA. Increasing NAA concentrations progressively inhibited primary root elongation of both wild-type and *35S::PID* plants, which were identified by the absence of lateral roots (Table 2). Inhibition of primary root growth in response to exogenous NAA indicated that auxin uptake into the root was not blocked by *PID* overexpression. However, exogenous NAA did not overcome the inhibition of lateral root growth, indicating that *35S::PID* plants were deficient specifically in lateral root formation.

Finally, to assay the effect of *PID* overexpression more directly, we crossed *35S::PID* to plants carrying the *DR5::GUS* reporter, which contains a multimerized synthetic auxin response element that is bound by ARF transcription factors (Ulmasov et al., 1997b; Sabatini et al., 1999). GUS activity in response to endogenous auxin in the root tips of *35S::PID* plants was reduced compared to plants that did not overexpress *PID* (Figures 5F

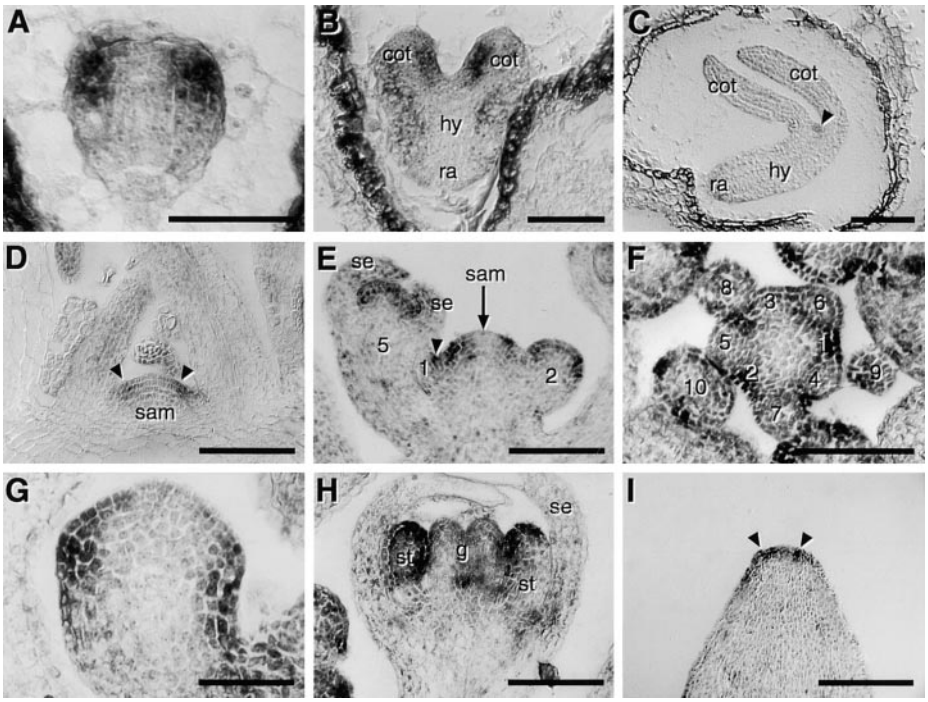

Figure 4. *PID* RNA Expression Determined by In Situ Hybridization

(A–H) Wild-type Columbia, except (F), which is Landsberg *erecta*. (A) *PID* expression first appears in the apical half of the globular stage embryo (Mansfield and Briarty, 1991; Jürgens and Mayer, 1993). (B) During the heart stage, expression becomes confined to the outer layers of the incipient cotyledons (cot), as well as the flanks of the presumptive hypocotyl (hy). It is absent from the embryonic root, the radicle (ra). (C) By the bent-cotyledon stage, only weak expression is detected in the shoot apical meristem (arrowhead). (D) During the vegetative phase, *PID* is expressed weakly (arrowheads) on the flanks of the shoot apical meristem (sam). (E) In the inflorescence, *PID* is expressed more strongly at the flanks of the shoot apical meristem, but has been excluded from most of a stage 1 flower, except for a small adaxial patch (arrowhead). Expression reappears on the flanks of a stage 2 flower. In the stage 5 flower, expression is apparent in the central floral meristem, but not in the outer whorl of sepals (se). (F) In this cross section of an inflorescence apex, floral anlagen (1, 2) and floral primordia (3–10) are consecutively numbered from youngest to oldest. Note exclusion of *PID* expression from the first apparent floral primordium ("3," stage 1 of flower development), and adaxial expression in flowers 4–6. (G) Close-up of an early stage 3 flower. (H) In a stage 7 flower, *PID* expression is apparent along the outer layers of the stamen (st) primordia, with lower levels in the central gynoecium (g). (I) *PID* expression in two small domains (arrowheads) on the flanks of the shoot apical meristem (arrowheads) of a *pin-1* inflorescence. Numbers indicate floral stages (Smyth et al., 1990), except for panel (F). Scale bars are 50 μm in (A), (B), and (G), and 100 μm in all other panels.

and 5G). Similarly, expression of the *DR5::GUS* reporter was repressed under inductive conditions. Exogenous auxin induces *DR5::GUS* expression in wild type (Ulmasov et al., 1997b; Sabatini et al., 1999), but growth of *35S::PID* seedlings on plates containing 0.1 μM NAA had little effect on *DR5::GUS* expression, which in wild-type plants marked developing lateral root primordia (Figures 5H and 5I). This result indicates that *PID* overexpression specifically blocked an early step in lateral root formation, rather than inhibiting lateral root outgrowth.

Discussion

PID Promotes Floral Meristem Outgrowth

Patterning of the shoot meristem proper is not grossly disrupted in *pid* mutants, as is evident from the normal expression patterns of the marker genes *CLV1* and *UFO* in the inflorescence meristem of *pid* mutants. Similarly, *FIL*, which marks the abaxial side of new floral primordia (Sawa et al., 1999; Siegfried et al., 1999), is expressed in *pid* mutants, even though its expression level is reduced. These data suggest that the primary defect during inflorescence development of *pid* mutants is the elaboration, rather than the establishment of lateral primordia. This is further supported by the phenotypic similarity between inflorescences of *pid* mutants and those of plants in which growth of floral primordia is arrested by flower-specific expression of a cellular toxin (Nilsson et al., 1998). The specific expression of *PID* RNA on the flanks of the inflorescence meristem indicates a local role of *PID* in promoting primordium outgrowth.

Although the expression pattern of *PID* in the embryo is similar to that seen in the inflorescence meristem, it is unclear whether its role in regulating growth of embryonic lateral primordia, the cotyledons, is the same as its role in regulating floral primordium growth. Whereas most flower primordia of *pid* mutants are growth arrested, cotyledons emerge normally in *pid* mutants, even though they are often affected in number and shape (Bennett et al., 1995). However, it is known that auxin signaling is required during the globular stage of embryogenesis to effect the transition from radial to bilateral symmetry at the time of cotyledon emergence (Sciavone and Cooke, 1987; Liu et al., 1993; Fischer and Neuhaus, 1996; Hadfi et al., 1998). The timing of this process correlates well with the expression of *PID* in

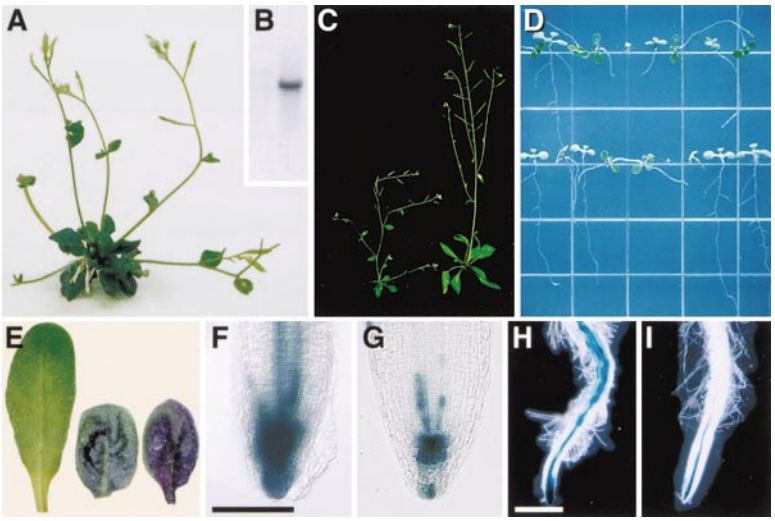

Figure 5. Phenotypes of *35S::PID* Plants

(A) 42-day-old *35S::PID* plant. Loss of apical dominance results in the simultaneous formation of multiple inflorescence shoots. (B) Northern blot hybridization with a *PID* cDNA probe of RNA from T1 transgenic plants that were phenotypically normal (left lane) or that showed a dominant phenotype (right lane). Each lane contained 12 μg of total RNA. (C) Wild-type (right) and *35S::PID* (left) plants. (D) Progeny of a hemizygous *35S::PID* plant segregated normal seedlings with numerous lateral roots and normal gravitropism and abnormal seedlings that lacked lateral roots and had short agravitropic roots. (E) Wild-type (left) and two *35S::PID* (right) rosette leaves. (F and G) Expression of the auxin-responsive *DR5:GUS* reporter (Ulmasov et al., 1997b) in root tips of wild-type (F) and *35S::PID* (G) plants. Scale bar is 50 μm for both panels. (H and I) Expression of the *DR5::GUS* reporter in roots of plants grown on 0.1 μM NAA. Strong GUS staining marks the emerging lateral root primordia in the wild-type root (H). Lateral root primordia are not detectable in *35S::PID* roots (I). Scale bar is 500 μm for both panels.

the presumptive cotyledons during the globular stage of embryogenesis. In contrast to the embryonic and reproductive phases, *PID* is only very weakly expressed in the vegetative apex and in young leaves, consistent with the absence of major vegetative defects in *pid* mutants (Bennett et al., 1995).

Vascular pattern defects in *pid* mutants similarly correlate with phases of *PID* expression. Unlike *mp* and *pin* mutants, which have decreased and excessive vascular proliferation in leaves, respectively (Przemeck et al., 1996; Mattsson et al., 1999), the vegetative tissues of *pid* mutants have normal venation. In contrast, petals and gynoecia in the flowers of *pid* mutants show vascular defects, consistent with the expression of *PID* in emerging floral organ primordia. Together, these observations suggest that *PID* regulates both the mitogenic effects of auxin in the control of lateral meristem outgrowth and its morphogenic effects during embryogenesis and vascular patterning.

Protein Kinases in Auxin Signaling

Previous studies have suggested the involvement of MAP kinase cascades in the regulation of auxin signaling. In vitro phosphorylation of a bacterially produced *Arabidopsis* MAP kinase by a tobacco cell extract is 3- to 4-fold more effective after treatment of protoplasts with the synthetic auxin 2,4-D, as compared to extracts from auxin-starved cultures (Mizoguchi et al., 1994). The importance of MAP kinase phosphorylation has also been demonstrated by overexpression in maize protoplasts of the catalytic domain of the tobacco MAPKK kinase NPK1, which blocks transcription from the auxin-responsive GH3 promoter (Kovtun et al., 1998). A role for protein phosphorylation in auxin transport has also been inferred from the discovery that the *Arabidopsis* gene *RCN1*, whose inactivation affects the response to the auxin transport inhibitor NPA, encodes a regulatory subunit of protein phosphatase 2A (Garbers et al., 1996).

PID encodes a protein kinase, but belongs to a different class of serine-threonine kinases than MAP, MAPK, or MAPKK kinases. PID contains 13 of the 14 invariant residues found in fungal and metazoan protein kinases (Hanks et al., 1988). The single exception is the replacement by aspartate of the invariant glycine of the DFG motif found in the consensus sequence of catalytic subdomain VII. The DFD motif of PID is present in several other putative plant kinases, and at least one of these, NPH1, which functions in blue-light mediated phototropism, also encodes a functional kinase (Christie et al., 1998).

Table 2. Root Growth in Response to Exogenous Auxin in *35S:PID* Plants

	Wild Type		*35S::PID*	
[NAA] (μM)	Root Length (mm)[a]	n	Root Length (mm)*	n
0	30.2 ± 7.0	13	15.5 ± 6.3	14
0.1	11.1 ± 1.7	15	7.6 ± 5.7	21
0.5	6.1 ± 1.0	11	6.0 ± 1.6	16
1	4.8 ± 1.6	12	4.6 ± 1.8	20

[a] Mean ± standard deviation.

PID Negatively Regulates Auxin Signaling

The exact roles of auxin in the development of the aerial parts of the plant are not well understood, making it difficult to precisely correlate mutant phenotypes with specific defects in auxin signaling. For example, while *pin* and *mp* mutant inflorescences are both defective in polar auxin transport (Okada et al., 1991; Przemeck et al., 1996), it is unclear whether the pin-phenotype of the inflorescence results from an excess or from a deficit in available auxin. Okada and colleagues (1991) have reported reduced free auxin levels at the whole plant level in *pin* mutants, but there is little information on

the local accumulation of auxin at the shoot apex or in developing lateral primordia of wild-type and mutant plants. In contrast, loss of lateral root formation has been directly linked to decreased levels of free auxin (Reed et al., 1998).

The phenotype of *35S::PID* plants supports the idea that *PID* negatively regulates auxin signaling. In the aerial part of the plant, *PID* overexpression results in dwarf stature, decreased apical dominance, and leaf curling. In the root, overexpression of *PID* leads to agravitropic growth and the absence of lateral roots. These phenotypes are characteristic of loss-of-function mutations in other genes believed to positively regulate auxin signaling, including *AXR1* and *TIR3* (Lincoln et al., 1990; Timpte et al., 1995; Ruegger et al., 1997). The proposed role for *PID* as a negative regulator of auxin response is confirmed molecularly by the decreased activity of the auxin-responsive *DR5::GUS* reporter in the root tips of *35S::PID* plants. Further support for this hypothesis comes from the observation that, unlike mutations that affect auxin transport or localization (Sabatini et al., 1999), *PID* overexpression does not alter the spatial pattern of *DR5::GUS* reporter expression. By extension, we propose that the pin-like inflorescence of *pin*, *mp*, and *pid* loss-of-function mutants is caused by increased auxin signaling. In contrast to *PID* overexpressers, *pid* mutants do not have an obvious root phenotype and respond normally to exogenous auxin (D. Smyth, personal communication), suggesting that in wild-type plants different *PID* homologs regulate tissue-specific auxin responses similar to the tissue-specific roles proposed for the *PIN/EIR1/AGR1* family of auxin transporters.

The Role of PID in Auxin Signaling

Besides mutations in the auxin transporter PIN, mutations in several ARF and Aux/IAA transcription factors, including ETTIN (ARF3), SHORT HYPOCOTYL 2 (IAA3), and MP (ARF5), cause phenotypes that are a subset of or overlap with *pid* loss-of-function phenotypes, suggesting that PID transmits auxin signals (Berleth and Jürgens, 1993; Bennett et al., 1995; Sessions and Zambryski, 1995; Tian and Reed, 1999). However, several other signaling pathways, such as those initiated by ethylene or ABA (Lehman et al., 1996; Luschnig et al., 1998; Ephritikhine et al., 1999), are known to affect auxin responses, and it remains to be seen whether PID merely modulates auxin signaling in response to other cues, or whether PID activity itself is regulated by auxin levels.

Experimental Procedures

Plant Growth

Plants were grown in florescent light (16 hr light, 8 hr dark). Wild type was Columbia. Transgenic plants were generated by vacuum infiltration (Bechtold et al., 1993). For root gravitropism experiments, seeds were grown on vertically oriented 1/2 × MS plates at 24°C.

In Situ Hybridization and Histological Analysis

Antisense probes for in situ hybridization were generated from pZL1-PID (*PID*); pDW221 (*UFO*) (Lee et al., 1997); the 5′ region of *FIL* in pBluescript (Siegfried et al., 1999); pAS66, which contains nucleotides 1165–1787 of the *CLV1* cDNA in pBluescript (a gift from A. Sessions); and three *MP* cDNA fragments in pSP72 (Hardtke and Berleth, 1998). Tissue preparation, hybridization and signal detection were essentially as described (Ferrándiz et al., 2000). Tissue for whole-mount analysis was prepared as described (Berleth and Jürgens, 1993), and viewed under dark-field illumination in a dissecting microscope. GUS assays were as described (Blázquez et al., 1997).

Cloning and Identification of *PID*

pid-9 genomic DNA was digested with HindIII (right border rescue) and BamHI (left border rescue), and plasmids were recovered as described (Weigel et al., 2000). Each *PID* exon was PCR amplified from genomic DNA of *pid* mutants, and after gel purification sequenced using an ABI DNA Sequencing Kit (Perkin Elmer).

cDNA Synthesis and Subcloning

RT-PCR was performed on total mRNA from inflorescences using the Reverse Transcription System Kit (Promega). First strand synthesis used an oligo dT primer. Subsequent PCR amplification used primers that amplified sequences from the initiation codon to 36 bp downstream of the stop codon. The products were cloned into the GST-fusion vector pGEX4T-1, and into the binary T-DNA vector CHF3, a derivative of pPZP212 (Hajdukiewicz et al., 1994) containing a CaMV 35S promoter/*nos* 3′ cassette and carrying the kanamycin resistance gene (a gift from C. Fankhauser). Mutations were introduced into the GST:PID and 35S::PID constructs by PCR with the QuikChange Site-Directed Mutagenesis Kit (Stratagene).

Protein Kinase Assays

Bacteria transformed with wild-type and mutant *GST::PID* constructs were induced with 1 mM IPTG when OD_{600} was 0.5 to 0.7. Culture was continued overnight at 18°C. After collecting the bacterial pellet by centrifugation, it was incubated on ice with extraction buffer (EB) (150 mM NaCl, 2 mM KCl, 2 mM KH_2PO_4, 10mM Na_2HPO_4, 2 mM EDTA, 2 mM DTT, 0.02% Pefabloc [Boehringer Mannheim]) for 30 min, followed by sonication for 2 min. Triton X-100 was added to 1%. The soluble fraction was isolated by spinning 10 min at 14,000 rpm in an Eppendorf centrifuge. 1.0 ml of the soluble fraction was added to 200 μl of a slurry of Glutathione agarose beads (Sigma) preequilibrated in EB and 1% Triton X-100, and tubes were rocked for 1 hr at 4°C. Beads were washed three times with EB and twice with HDE (20 mM HEPES, 5 mM DTT, 5 mM EDTA). For kinase assays, 10 μl of glutathione beads containing the bound protein were mixed with 4 μl 5× kinase buffer (125 mM Tris, pH 7.5, 25 mM $MgCl_2$, 1 mM EDTA), 1 μl [γ-^{32}P]ATP (specific concentration 3000 Ci/mM), 0.2 μl 10 mM ATP, and 4.8 μl dH_2O, and incubated for 30 min at 30°C. After extensive washes with EB, one volume of FSB (250 mM Tris/HCl pH 6.8, 2% SDS, 30% glycerol, 0.1 M DTT, 0.02% bromophenol blue) was added to each sample. Samples were boiled and spun briefly, and 15 μl of the supernatant was separated on precast 4%–15% polyacrylamide gels (BIO-RAD).

Acknowledgments

We are grateful to D. Smyth for discussion and communicating unpublished results. We thank J. Fletcher, R. Hong, A. Sessions, D. Smyth, J. Murfett, and T. Guilfoyle for seeds; J. Bowman, A. Sessions, T. Berleth, C. Fankhauser, K. Palme, and L. Gälweiler for plasmids; A. Sessions, G. Gocal, and P. Pinyopich for help with in situ hybridization; M. Blázquez, M. Estelle, and A. Sessions for helpful comments on the manuscript; and members of the Chory and Weigel labs, especially P. Gil, for valuable discussion. This work was supported by an NSF Postdoctoral Fellowship (S. K. C.), and by grants from the DOE (DE-FG03–89ER13993 to J. C.) and NSF (MCB-9631390 to J. C. and IBN-9723818 to D. W.). J. C. is an Associate Investigator of the Howard Hughes Medical Institute and D. W. was an NSF Young Investigator.

Received November 11, 1999; revised January 19, 2000.

References

Aloni, R. (1995). The induction of vascular tissues by auxin and cytokinin. In Plant Hormones: Physiology, Biochemistry and Molecular Biology, P.J. Davies, ed. (Netherlands: Kluwer Academic Publishers), pp. 531–545.

Bechtold, N., Ellis, J., and Pelletier, G. (1993). *In planta Agrobacterium* mediated gene transfer by infiltration of adult *Arabidopsis thaliana* plants. C. R. Acad. Sci. *316*, 1194–1199.

Bennett, S.R.M., Alvarez, J., Bossinger, G., and Smyth, D.R. (1995). Morphogenesis in *pinoid* mutants of *Arabidopsis thaliana*. Plant J. *8*, 505–520.

Bennett, M.J., Marchant, A., Green, H.G., May, S.T., Ward, S.P., Millner, P.A., Walker, A.R., Schulz, B., and Feldmann, K.A. (1996). *Arabidopsis AUX1* gene: a permease-like regulator of root gravitropism. Science *273*, 948–950.

Berleth, T., and Jürgens, G. (1993). The role of the *monopteros* gene in organising the basal body region of the *Arabidopsis* embryo. Development *118*, 575–587.

Blázquez, M.A., Soowal, L., Lee, I., and Weigel, D. (1997). *LEAFY* expression and flower initiation in *Arabidopsis*. Development *124*, 3835–3844.

Celenza, J.L., Jr., Grisafi, P.L., and Fink, G.R. (1995). A pathway for lateral root formation in *Arabidopsis thaliana*. Genes Dev. *9*, 2131–2142.

Chen, R., Hilson, P., Sedbrook, J., Rosen, E., Caspar, T., and Masson, P.H. (1998). The *Arabidopsis thaliana AGRAVITROPIC 1* gene encodes a component of the polar-auxin-transport efflux carrier. Proc. Natl. Acad. Sci. USA *95*, 15112–15117.

Christie, J.M., Reymond, P., Powell, G.K., Bernasconi, P., Raibekas, A.A., Liscum, E., and Briggs, W.R. (1998). *Arabidopsis* NPH1: a flavoprotein with the properties of a photoreceptor for phototropism. Science *282*, 1698–1701.

Clark, S.E., Williams, R.W., and Meyerowitz, E.M. (1997). The *CLAVATA1* gene encodes a putative receptor kinase that controls shoot and floral meristem size in Arabidopsis. Cell *89*, 575–585.

Davies, P.J. (1995). The plant hormones: their nature, occurrence, and functions. In Plant Hormones: Physiology, Biochemistry and Molecular Biology, P.J. Davies, ed. (Netherlands: Kluwer Academic Publishers), pp. 1–12.

Ephritikhine, G., Fellner, M., Vannini, C., Lapous, D., and Barbier-Brygoo, H. (1999). The *sax1* dwarf mutant of *Arabidopsis thaliana* shows altered sensitivity of growth responses to abscisic acid, auxin, gibberellins and ethylene and is partially rescued by exogenous brassinosteroid. Plant J. *18*, 303–314.

Ferrándiz, C., Gu, Q., Martienssen, R., and Yanofsky, M.F. (2000). Redundant regulation of meristem identity and plant architecture by *FRUITFULL*, *APETALA1* and *CAULIFLOWER*. Development *127*, 725–734.

Fischer, C., and Neuhaus, G. (1996). Influence of auxin on the establishment of bilateral symmetry in monocots. Plant J. *10*, 659–667.

Gälweiler, L., Guan, C., Müller, A., Wisman, E., Mendgen, K., Yephremov, A., and Palme, K. (1998). Regulation of polar auxin transport by AtPIN1 in *Arabidopsis* vascular tissue. Science *282*, 2226–2230.

Garbers, C., DeLong, A., Deruére, J., Bernasconi, P., and Söll, D. (1996). A mutation in protein phosphatase 2A regulatory subunit A affects auxin transport in *Arabidopsis*. EMBO J. *15*, 2115–2124.

Gray, W.M., del Pozo, J.C., Walker, L., Hobbie, L., Risseeuw, E., Banks, T., Crosby, W.L., Yang, M., Ma, H., and Estelle, M. (1999). Identification of an SCF ubiquitin-ligase complex required for auxin response in *Arabidopsis thaliana*. Genes Dev. *13*, 1678–1691.

Guilfoyle, T., Hagen, G., Ulmasov, T., and Murfett, J. (1998). How does auxin turn on genes? Plant Physiol. *118*, 341–347.

Hadfi, K., Speth, V., and Neuhaus, G. (1998). Auxin-induced developmental patterns in *Brassica juncea* embryos. Development *125*, 879–887.

Hajdukiewicz, P., Svab, Z., and Maliga, P. (1994). The small, versatile pPZP family of *Agrobacterium* binary vectors for plant transformation. Plant Mol. Biol. *25*, 989–994.

Hanks, S.K., Quinn, A.M., and Hunter, T. (1988). The protein kinase family: conserved features and deduced phylogeny of the catalytic domains. Science *241*, 42–52.

Hardtke, C.S., and Berleth, T. (1998). The *Arabidopsis* gene *MONOPTEROS* encodes a transcription factor mediating embryo axis formation and vascular development. EMBO J. *17*, 1405–1411.

Jones, A.M., Im, K.H., Savka, M.A., Wu, M.J., DeWitt, N.G., Shillito, R., and Binns, A.N. (1998). Auxin-dependent cell expansion mediated by overexpressed auxin-binding protein 1. Science *282*, 1114–1117.

Jürgens, G., and Mayer, U. (1993). *Arabidopsis*. In A Colour Atlas of Developing Embryos, J. Bard, ed. (London: Wolfe Publ.), pp. 7–21.

Kaufman, P.B., Wu, L.-L., Brock, T.G., and Kim, K. (1995). Hormones and the orientation of growth. In Plant Hormones: Physiology, Biochemistry and Molecular Biology, P.J. Davies, ed. (Netherlands: Kluwer Academic), pp. 547–570.

Kim, J., Harter, K., and Theologis, A. (1997). Protein-protein interactions among the Aux/IAA proteins. Proc. Natl. Acad. Sci. USA *94*, 11786–11791.

Kovtun, Y., Chiu, W.L., Zeng, W., and Sheen, J. (1998). Suppression of auxin signal transduction by a MAPK cascade in higher plants. Nature *395*, 716–720.

Lammer, D., Mathias, N., Laplaza, J.M., Jiang, W., Liu, Y., Callis, J., Goebl, M., and Estelle, M. (1998). Modification of yeast Cdc53p by the ubiquitin-related protein Rub1p affects function of the SCF^{Cdc4} complex. Genes Dev. *12*, 914–926.

Lee, I., Wolfe, D.S., Nilsson, O., and Weigel, D. (1997). A *LEAFY* coregulator encoded by *UNUSUAL FLORAL ORGANS*. Curr. Biol. *7*, 95–104.

Lehman, A., Black, R., and Ecker, J.R. (1996). *HOOKLESS1*, an ethylene response gene, is required for differential cell elongation in the Arabidopsis hypocotyl. Cell *85*, 183–194.

Leyser, H.M.O., Pickett, F.B., Dharmasiri, S., and Estelle, M. (1996). Mutations in the *AXR3* gene of *Arabidopsis* result in altered auxin response including ectopic expression from the SAUR-AC1 promoter. Plant J. *10*, 403–413.

Liakopoulos, D., Doenges, G., Matuschewski, K., and Jentsch, S. (1998). A novel protein modification pathway related to the ubiquitin system. EMBO J. *17*, 2208–2214.

Lincoln, C., Britton, J.H., and Estelle, M. (1990). Growth and development of the *axr1* mutants of Arabidopsis. Plant Cell *2*, 1071–1080.

Liu, C., Xu, A., and Chua, N. (1993). Auxin polar transport is essential for the establishment of bilateral symmetry during early plant embryogenesis. Plant Cell *5*, 621–630.

Long, J.A., and Barton, M.K. (1998). The development of apical embryonic pattern in *Arabidopsis*. Development *125*, 3027–3035.

Luschnig, C., Gaxiola, R.A., Grisafi, P., and Fink, G.R. (1998). EIR1, a root-specific protein involved in auxin transport, is required for gravitropism in *Arabidopsis thaliana*. Genes Dev. *12*, 2175–2187.

Maher, E.P., and Martindale, S.J. (1980). Mutants of *Arabidopsis thaliana* with altered responses to auxins and gravity. Biochem. Genet. *18*, 1041–1053.

Mansfield, S.G., and Briarty, L.G. (1991). Early embryogenesis in *Arabidopsis thaliana*. II. The developing embryo. Can. J. Bot. *69*, 461–476.

Marchant, A., Kargul, J., May, S.T., Muller, P., Delbarre, A., Perrot-Rechenmann, C., and Bennett, M.J. (1999). AUX1 regulates root gravitropism in *Arabidopsis* by facilitating auxin uptake within root apical tissues. EMBO J. *18*, 2066–2073.

Mattsson, J., Sung, Z.R., and Berleth, T. (1999). Responses of plant vascular systems to auxin transport inhibition. Development *126*, 2979–2991.

Mizoguchi, T., Gotoh, Y., Nishida, E., Yamaguchi-Shinozaki, K., Hayashida, N., Iwasaki, T., Kamada, H., and Shinozaki, K. (1994). Characterization of two cDNAs that encode MAP kinase homologues in *Arabidopsis thaliana* and analysis of the possible role of auxin in activating such kinase activities in cultured cells. Plant J. *5*, 111–122.

Müller, A., Guan, C., Gälweiler, L., Tanzler, P., Huijser, P., Marchant, A., Parry, G., Bennett, M., Wisman, E., and Palme, K. (1998). *AtPIN2* defines a locus of *Arabidopsis* for root gravitropism control. EMBO J. *17*, 6903–6911.

Nilsson, O., Wu, E., Wolfe, D.S., and Weigel, D. (1998). Genetic ablation of flowers in transgenic *Arabidopsis*. Plant J. *15*, 799–804.

Odell, J.T., Nagy, F., and Chua, N.-H. (1985). Identification of DNA-sequences required for activity of the cauliflower mosaic virus-35S promoter. Nature *313*, 810–812.

Okada, K., Ueda, J., Komaki, M.K., Bell, C.J., and Shimura, Y. (1991). Requirement of the auxin polar transport system in early stages of *Arabidopsis* floral bud formation. Plant Cell *3*, 677–684.

Patton, E.E., Willems, A.R., Sa, D., Kuras, L., Thomas, D., Craig, K.L., and Tyers, M. (1998). Cdc53 is a scaffold protein for multiple Cdc34/Skp1/F-box protein complexes that regulate cell division and methionine biosynthesis in yeast. Genes Dev. *12*, 692–705.

Przemeck, G.K.H., Mattsson, J., Hardtke, C.S., Sung, Z.R., and Berleth, T. (1996). Studies on the role of the *Arabidopsis* gene *MONOPTEROS* in vascular development and plant cell axialization. Planta *200*, 229–237.

Reed, R.C., Brady, S.R., and Muday, G.K. (1998). Inhibition of auxin movement from the shoot into the root inhibits lateral root development in Arabidopsis. Plant Physiol. *118*, 1369–1378.

Rouse, D., Mackay, P., Stirnberg, P., Estelle, M., and Leyser, O. (1998). Changes in auxin response from mutations in an *AUX/IAA* gene. Science *279*, 1371–1373.

Ruegger, M., Dewey, E., Hobbie, L., Brown, D., Bernasconi, P., Turner, J., Muday, G., and Estelle, M. (1997). Reduced naphthylphthalamic acid binding in the *tir3* mutant of Arabidopsis is associated with a reduction in polar auxin transport and diverse morphological defects. Plant Cell *9*, 745–757.

Sabatini, S., Beis, D., Wolkenfelt, H., Murfett, J., Guilfoyle, T., Malamy, J., Benfey, P., Leyser, O., Bechtold, N., Weisbeek, P., and Scheres, B. (1999). An auxin-dependent distal organizer of pattern and polarity in the *Arabidopsis* root. Cell *99*, 463–472.

Sawa, S., Watanabe, K., Goto, K., Kanaya, E., Morita, E.H., and Okada, K. (1999). *FILAMENTOUS FLOWER*, a meristem and organ identity gene of *Arabidopsis*, encodes a protein with a zinc finger and HMG-related domains. Genes Dev. *13*, 1079–1088.

Sciavone, F.M., and Cooke, T.J. (1987). Unusual patterns of somatic embryogenesis in the domesticated carrot: developmental effects of exogenous auxins and auxin transport inhibitors. Cell Differ. *21*, 53–62.

Sessions, R.A., and Zambryski, P.C. (1995). *Arabidopsis* gynoecium structure in the wild type and in *ettin* mutants. Development *121*, 1519–1532.

Siegfried, K.R., Eshed, Y., Baum, S.F., Otsuga, D., Drews, G.N., and Bowman, J.L. (1999). Members of the YABBY gene family specify abaxial cell fate in *Arabidopsis*. Development *126*, 4117–4128.

Smyth, D.R., Bowman, J.L., and Meyerowitz, E.M. (1990). Early flower development in *Arabidopsis*. Plant Cell *2*, 755–767.

Tian, Q., and Reed, J.W. (1999). Control of auxin-regulated root development by the *Arabidopsis thaliana SHY2/IAA3* gene. Development *126*, 711–721.

Timpte, C., Lincoln, C., Pickett, F.B., Turner, J., and Estelle, M. (1995). The *AXR1* and *AUX1* genes of *Arabidopsis* function in separate auxin-response pathways. Plant J. *8*, 561–569.

Ulmasov, T., Hagen, G., and Guilfoyle, T.J. (1997a). ARF1, a transcription factor that binds to auxin response elements. Science *276*, 1865–1868.

Ulmasov, T., Murfett, J., Hagen, G., and Guilfoyle, T.J. (1997b). Aux/IAA proteins repress expression of reporter genes containing natural and highly active synthetic auxin response elements. Plant Cell *9*, 1963–1971.

Ulmasov, T., Hagen, G., and Guilfoyle, T.J. (1999). Dimerization and DNA binding of auxin response factors. Plant J. *19*, 309–319.

Weigel, D., Alvarez, J., Smyth, D.R., Yanofsky, M.F., and Meyerowitz, E.M. (1992). *LEAFY* controls floral meristem identity in Arabidopsis. Cell *69*, 843–859.

Weigel, D., Ahn, J.H., Blázquez, M.A., Borevitz, J., Christensen, S.K., Fankhauser, C., Ferrándiz, C., Kardailsky, I., Malancharuvil, E.J., Neff, M.M., Nguyen, J.T., Sato, S., Wang, Z., Xia, Y., Dixon, R.A., Harrison, M.J., Lamb, C.J., Yanofsky, M.F., and Chory, J. (2000). Activation tagging in Arabidopsis. Plant Physiol., in press.

GenBank Accession Number

The PINOID cDNA sequence has been deposited in GenBank under accession number AF232236.